CIRCULATION COPY
SUBJECT TO RECALL
IN TWO WEEKS

THE MOON AS A CALIBRATION TARGET
OF CONVENIENCE FOR
VHF - UHF RADAR SYSTEMS

J. D. Mathews
J. K. Breakall
M. P. Sulzer

THIS PAPER WAS PREPARED FOR SUBMITTAL TO

Radio Science

Lawrence
Livermore
National
Laboratory

DISCLAIMER

The Moon as a Calibration Target of Convenience for VHF - UHF Radar Systems

J. D. Mathews[1], J. K. Breakall[2], and M. P. Sulzer[3]

Abstract

Knowledge of the absolute, versus relative, performance characteristics of VHF and UHF radars used in geophysical applications is often important. We suggest that the moon may form a convenient, easily tracked calibration target for many such radars. The lunar absolute radar scattering cross-section is large, well known (~7% of the visible disk) and is essentially wavelength independent over $6m > \lambda > 1cm$. We develop and present the radar equation appropriate to this calibration process and give the results of calibrating the Arecibo 430 MHz radar in this manner.

[1] Electromagnetic Waves and Wave Propagation Group, Dept. of Electrical Engineering and Applied Physics, Case Institute of Technology, Case Western Reserve University, Cleveland, Ohio

[2] University of California, Lawrence Livermore National Laboratory, P. O. Box 808, Livermore, CA 94550

[3] National Astronomy and Ionosphere Center, Arecibo Observatory, P. O. Box 995, Arecibo, Puerto Rico 00613

I. INTRODUCTION

It is often convenient and even necessary to verify the performance of a radar system in an absolute sense. An example of current interest involves the so-called ST or MST (Mesospheric, Stratospheic, Tropospheric) radars [Harper and Gordon, 1980] for which absolute scattering cross-sections per unit volume from these atmospheric regions could prove valuable [e.g., Rottger, 1980]. Unfortunately, the complexity of these and similar systems [e.g., the Arecibo 430 MHz Incoherent Scatter Radar (ISR) system] make absolute calibration of the total system done by calibrating the individual subsystems difficult and subject to cumulative errors. However, if a radar target of relatively simple known characteristics were available each radar system could be regularly checked and inter-compared. This was the intent of the 1 m^2 optical cross-section Lincoln Calibration Sphere (LCS) launched into a 1500 km almost circular orbit in 1965 [Prosse, 1965]. Unfortunately, the LCS and similar targets pose a tracking and system sensitivity problem for simple radars and degrade from micrometer collisions over time.

An easily tracked, well characterized alternative target which is visible to some MST and ISR radars is the moon. The moon has been the subject of intense investigation by radar astronomers for many years [e.g., Hagfors and Evans, 1968] and is still the subject of considerable interest [Thompson, 1979; Tyler, 1979; Simpson and Tyler, 1982]. This work has led to excellent determinations of the total lunar radar scattering cross-section. This cross-section, σ_0, is about 0.071π r_ℓ^2 (r_ℓ is the lunar radius) and is nearly frequency independent for 6 m$\geq \lambda \geq$1 cm [Evans and Pettengill, 1963 a,b; Evans and Hagfors, 1966; Evans, 1969; Burns, 1970]. Monostatic radar scattering from the moon is dominated by the small region of the moon directly "below" the radar, the subradar point. Scattering from the subradar region is termed quasi-specular in that it arises from the almost "smooth" (i.e., surfaces which are flat compared with probing wavelength, of area of order λ^2 or larger and with surface normals parallel or nearly parallel to the radar wave vector) regions within the subradar region [Hagfors and Evans, 1968; Simpson, 1976]. Total cross-section results do however depend on the location of the subradar point on the moon [Burns, 1970] and, at longer wavelengths, on careful accounting for ionospheric Faraday rotating effects if linear polarization is used [Hagfors and Evans, 1968]. More will be said about σ_0 as we derive and employ it in later section.

The idea of using the moon as a reasonably general calibration target occurred as a result of an attempt to calibrate the Arecibo 430 MHz radar system for absolute measurements of power scattered incoherently from the ionosphere [e.g., Mathews, 1984, 1985]. This attempt required careful determinations of the antenna pattern [Breakall and Mathews, 1982; Breakall, 1983] as well as transmitted power and overall system performance. We choose to employ the moon as a calibration target to first compare the high power transmitter performance with that of a low power, well characterized reference transmitter and secondly to determine the total lunar scattering cross-section for comparison with earlier work. These tasks were successful and are reported here.

Section 2 of this paper is devoted to the various forms of the radar equation derived in Appendix A while Section 3 contains the results of applying the radar equation to the Arecibo 430 MHz moon bounce experiment. Section 4 is a summary and general discussion of how the moon may be used as a VHF-UHF calibration target.

II. *RADAR LUNAR CALIBRATION PROCEDURES*

The calibration procedure we describe requires only total scattered power as a function of time (pulsed radar mode) assuming that the radar is tracking the nearest point on the moon (the subradar point). An appropriate form of the lunar radar equation is derived in Appendix A with experiment geometry given in Fig. A1. For a simple wide antenna beam (beam full width at half maximum greater than the $1/2°$ lunar apparent "size") radar operated in quasi-CW mode ("square" pulse lengths approaching 11.6 msec) the total (i.e., peak) received power is given by (A12) as

$$P_R = \frac{\lambda^2 L P_o G_o^2}{(4\pi)^3 R^4} \sigma_o \qquad (1)$$

where R, the radar-subradar point distance, is approximately 3.76×10^8m while σ_o, the total lunar radar scattering cross-section is about 0.071±0.018 (+1.2 dB, -1.3 dB) [Evans and Hagfors, 1968; average of Table 5-2 results for 0.86 cm≤ λ ≤784 cm less the 12.5 cm result] the projected area of the moon. When P_R is determined absolutely by comparing the relative received power with a noise calibration standard (i.e., $P_N = \kappa T_c B$ = noise power; κ = Boltzmann's constant, T_c = calibration source temperature, B = noise bandwidth) (1) yields $LP_o G_o^2$.

The conditions required for (1) to obtain seldom occur. For example, the antenna beam maybe wide compared with the moon but the transmitter used may not provide a quasi-CW mode or the long pulse provided may decay in power due to power supply "droop". In this case (A11) is used with $P_n(\Theta) \simeq 1$ (wide beam) yielding

$$P_R(t) = \frac{\lambda^2 L P_o G_o^2}{(4\pi)^3 R^4} \sigma_o W(t) \qquad (2)$$

The pulse/lunar weighting function W(t) is defined as

$$W(t) = \frac{1}{\Gamma} \int_o^{\tau_\ell} e^{-(t-t')/\tau_\iota} [s(t'-t+\Delta) - s(t-t')] \gamma_n(t') \pi c r_\ell dt' \qquad (3)$$

where various terms are defined in Appendix A and we assume an exponentially decaying pulse of length Δ (any pulse shape can be used). The normalized scattering cross-section γ_n is defined in equations (A13) and (A14) in terms of very short pulse, wide beam scattering from the moon.

3

It is clear from (3) that unless (1) obtains the normalized cross-sections $\gamma_n(t)$ is needed for the wavelength of the radar in question. If the "wide-beam" approximation applies $\gamma_n(t)$ maybe measured directly if sufficient signal-to-noise ratio is available to make this approach viable (note that this measurement if successful immediately "calibrates" the radar via equations (A9), (A10), and (A13)). Fortunately, however, γ_n is available from the literature for several wavelengths of interest. Representative results are given in Figs. 5-9, 10 of Evans and Hagfors [1968]. Tabulated γ_n versus delay (or lunar angle α) are given for $\lambda = 3.8$, 23, and 68 cm by Hagfors [1967, Table 1; 1970, Table 6].

An analytic formula for γ_n is given by Beckman [1965] and in his references. This analytic form, which is remarkably accurate (± 1dB), is in terms of lunar angle $\alpha = \alpha(t)$ (see Fig. A1 and equation (A4)) and is

$$\gamma_n(\alpha) = \{cos^4\alpha + C\ sin^2\alpha\}^{-\frac{3}{2}} \cdot exp\left[-\frac{1}{4}\ tan\ \alpha\ erfc\ (K\ cot\ \alpha)\right] \qquad (4)$$

where

$$erfc(x) = \frac{2}{\sqrt{\pi}}\int_x^\infty e^{-t^2}dt$$

and where "constants" C and K are wavelength dependent. In (4) the polynomial term describes the quasi-specular component of scattering which comes from the "smooth" structures in the subradar region. The exponential term describes the "diffuse" scattering component which arises from irregular surface features and is dominant for larger α values. That is, at light frequencies the diffuse component is totally dominant (i.e., no bright spot) and the surface appears to be uniformly bright while at $\lambda = 68$ cm the subradar region is "bright" (the quasi-specular component contribute 83% of the total scattering cross-section, Evans and Hagfors, 1968, section 5.4) compared with the "limb" regions. The subradar region becomes even brighter relative to the limb regions at meter wavelengths [e.g., see Klemperer, 1965]. Values of C and K from (4) are given in Table 1 for a few wavelength values.

Finally a "worst case" calibration involves no simplifications to (A11). This is the situation with the Arecibo 430 MHz incoherent scatter radar system which has a half-power beam width of $1/6°$ which is considerable less than the $1/2°$ apparent angular size of the moon. We consider the full calibration of the Arecibo system in the next section.

III. *THE ARECIBO 430 MHz RADAR SYSTEM CALIBRATION*

The procedures we describe here were designed to measure the absolute performance characteristics of the Arecibo 430 MHz radar as a total system (receiver, transmitter, antenna) and of the main transmitter as a separate system component. To this end we used both the main, high power ($\sim$2.0 MWatt) transmitter and a well characterized low

power (5.9 Watt) reference transmitter to illuminate the moon as the sub-radar point on the moon was "tracked". The full form of the radar equation, (A11) must be used in this case due to the narrow beamwidth of the 61.1 dBi gain antenna. Thus the antenna pattern is needed in order to interpret these measurements in terms of (A11). The pattern has been obtained both theoretically and experimentally as described by Breakall and Mathews [1982].

The low power transmitter was connected to the antenna feed at the turnstile junction [Meyer and Goldberg, 1955] thus avoiding losses in 1300 feet of waveguide as well as slight coupling losses. The parametric amplifier "front-end" was, because of large signal strengths, isolated from the feed by 20.99 dB or 71.59 dB attenuation during use of the low and high power transmitters respectively. Waveguide loss was measured to be 1.25 dB for the main transmitter and a 9.78 kHz noise bandwidth Gaussian IF filter was used in the receiver system. Transmitter pulse length was 2 msec (decaying exponentials as will be discussed) with a 101.6 msec interpulse period (IPP). The lunar distance at the time of the experiment was about 3.674×10^5 km yielding a pulse travel time of 2.45 sec. Thus 24 pulses were transmitted before a particular pulse was received. The IPP was adjusted so that returning pulses arrived at a time when the receiver could be conveniently gated on. The parameters of the experiment are listed in Table 2.

This experiment was performed on 28 October 1980 when the moon passed within $2°$ of zenith at 042736 hrs local time (66° 45.2'W, 18° 20'36.6"N). The low power transmitter was used from 0347-0406 hrs (before transit) and the high power transmitted was used from 0454-0510 hrs (after transit). During these periods data was accumulated (averaged) for 500 IPP's (~50 secs) and then written on magnetic tape.

Analysis of this data takes two forms. First the two sets of results are compared to determine the relative performance of the two transmitters. Secondly, via (A11), total system performance is evaluated and our assumptions concerning the form of γ_n [see(4)] are tested.

The two transmitters are compared on a relative basis by determining the "best" signal-to-noise ratios for each observing mode; adjusting these ratios to account for differing receiver attenuation, and then taking the ratio of the resultant SNR's where noise level is the same for both modes. The SNR for each mode is determined as indicated in Fig. 1. Figure 1 shows the received, lunar scattered radar pulse in a 4.5 msec long segment of the 50 msec "observing window" used in this work. This return, which is from the 1.7 MWatt transmitter, is the result of accumulating (summing) 500 IPP's (50.8 secs, 1 tape write) of results which were sampled every 50 μsecs for 1000 range gates. The solid lines are average values of the baseline excluding the pulse and of the pulse peak (the 30 samples starting 0.5 msec "into" the pulse are averaged) while the dashed lines are at the 1 and 5 standard deviation level for the pulse peak and baseline respectively. The ratio of the peak-to-baseline value is the SNR for each 500 IPP sample. Note that the error

in the estimate of the SNR is dominated by the "noise" at the pulse peak. This noise is dominated by interference effects (fading) among various lunar scattering centers as the subradar location moves across the lunar surface due, mostly, to the earth's rotation [lunar libration; Evans and Hagfors, 1968; section 5-3].

Errors in SNR estimates are lessened by averaging together all SNR estimates for the low and all high power transmitter modes respectively. Before this was done a small zenith angle correction to the gain was applied to each 500 IPP estimate of the SNR. This correction (which references the SNR to 0° zenith angle) arises from the fact that at Arecibo "pointing" is achieved by moving the feed (resulting in imperfect illumination of the spherical disk at larger zenith angles) rather than the entire structure. The total correction, obtained from radio astronomical observations, is very accurate and amounts to a maximum of 1 dB gain correction or 2 dB shift in SNR (see (A11)). The resultant SNR's, before removal of receiver attenuation, are (see Table 2) 5.5 ± 0.5 and 10.2 ± 1.0 for the low and high power transmitted respectively. After removal of the 50.6 dB difference in receiver attenuation we find the high power transmitter delivered 1.256 MW at the feed or 1.68 MW after removal of waveguide losses. This measurement confirmed the validity of the bolometer power measurements.

The radar system absolute properties are determined via (A11) and using the final SNR values converted to absolute power. The system temperature was determined, by use of a calibration noise source, to be $T_{sys} = 339$ K. The system noise bandwidth was 9.78 kHz thus absolute noise power is

$$P_N = \kappa T_{sys} B \cdot (SNR) \tag{5}$$

where κ is Boltzmann's constant. Average signal power at the pulse peak (see Fig. 1) is then 3.16×10^{-14} Watts and 6.73×10^{-9} Watts for the low and high power transmitters respectively.

As is clear from (A11) we must determine Γ (see (A10)) and evaluate $P_R(t)$ at the pulse peak in order to interpret received absolute power levels in terms of the lunar radar cross-section. In Fig. 2 the normalized antenna pattern squared and γ_n (the 68 cm result from Hagfors (1967) Table 1) are plotted versus the "distance" into the moon measured in round-trip travel time assuming that the subradar point is being tracked. Note that γ_n falls off much more steeply than p_n^2 clearly indicating that even the Arecibo radar "sees" the moon as an angularly unresolved bright spot which is distinguishable only by high time resolution measurements. The integral of $\gamma_n(t')$ as defined by (A10) is $\Gamma = 1.4301$ $(-4) \cdot \pi c r_\ell$. The integral of the product of γ_n and p_n^2 is about 0.52 Γ indicating (see A11) that a maximum of 0.52 of the lunar scattering cross-section is "visible" to the A0 radar even in the quasi-CW case.

As a measure of the validity of γ_n as chosen we compare the theoretical $P_R(t)$ with the highly averaged low and high power transmitter derived return pulses. In Fig. 3a, b we show these pulses along with two "predicted" pulses for each case. The theoretical curves marked $\tau_t \to \infty$ assume an ideal "square" transmitter pulse and asymptotically approach the value of the quasi-CW case. However the measured returns display a peak and then decay slowly until t=2 msec after which the expected steep decline occurs. This type return is characteristic of transmitter "droop" during the pulse. Unfortunately we did not realize the existence of this problem during the experiment. However, later measurements confirmed the basic exponential behavior which we assume in (A11).

The theoretical curves in Fig. 3 which closely resemble the measured results assume low and high power transmitter time constants of 16 msec and 30 msec respectively. These time constants were determined by comparing a family of theoretical curves with the experimental results. No formal fitting procedure was used since γ_n has also been assumed. Despite these difficulties the quality of the "fit" of the theoretical to experimental curves indicates the basic validity of our approach and allows for a determination of σ_0 using (A11) and the average signal power at the peak of the return pulses. Also different γ_n curves were tried in order to test the sensitivity of our results to γ_n. We found that use of (4) with the Table 1 68 cm coefficients resulted in an $\sim$1% change in inferred σ_0 while use of the 23 cm coefficients produced only a 15% (0.6 dB) increase in σ_0.

The final averaged signal powers are based on averaging the 30 samples obtained 0.5 msec after the start of the pulse. The equivalent average of the $P_R(t)$ curves of Fig. 3 is expressed as the average of $W(t)$ (given by (3)) and is $\overline{W} = 0.479$ and $\overline{W} = 0.496$ for the low and high power transmitters respectively (see Table 3). These results represent minor deviations from an ideal square pulse for which $\overline{W} = 0.516$. The apparent lunar cross-section is now easily obtained from the measurements using both transmitters by inverting (2) utilizing the data from Tables 2 and 3. The final cross-sections, given as fractions of πr_ℓ^2, are 0.054 and 0.051 for the low and high power transmitters.

The lunar cross-section values determined here compare quite favorably with those in the literature. In fact, except for having to use γ_n from the literature we feel that the total cross-section determination is, because of using the two transmitters and a very good antenna pattern, correct to within $\pm$20% including systematic errors. The caveat here is that although the $\gamma_n(t)$ used gives a good match between expected and observed signal temporal behavior additional systematic error is possible. For example the very narrow (in time) leading edge of the $\gamma_n(t)$ curve maybe unresolved leading to slightly large $\overline{W}$ values thus causing σ_0 to be underestimated. However, our cross-section determination clearly confirms that the Arecibo 430 MHz radar is behaving as expected even though our σ_0 maybe somewhat low in value. Thus even in this "worst case" situation of a radar in which the full equation (A11) must be used it has been relatively easy to perform the lunar calibration study.

7

IV. DISCUSSION AND SUMMARY

Absolute calibration of a radar system can be difficult and especially in circumstances where results from two or more widely separated radars are to be compared a common calibration target would be useful. We suggest that the moon which has been previously determined to have a radar cross-section of about 7% of its projected area over 50–3000 MHz may be an acceptable target. The large scattering cross-section makes the moon visible to even small radars or communication systems [Reisert, 1982]. Also, the small angular rate of motion, relative to near earth satellites, of the moon across the sky allows for easy tracking. In the case of the Arecibo experiment described here, tracking was accomplished via a computer code derived from the American Ephemeris and Nautical Almanac and on the Explanatory Supplement to the Ephemeris. Copies of this code are available on request.

There are, however, difficulties, especially for VHF radars, associated with using the moon as a radar target. The major problem is probably that the moon goes overhead only between the latitudes of about ±28.5°. Thus may of the midlatitude MST radars which are not steerable or are only steerable over a small range of angles near zenith are denied this target. A second problem involves fading of the return signal due to the varying interference of signal components from various lunar features as the subradar point wanders across the lunar surface [lunar libration; Hagfors and Evans, 1968]. This fading effect must be averaged out in order to find the mean return pulse from which (assuming σ_o) the radar system is calibrated.

A similar problem is fading of the signal due to the Faraday rotation which occurs in the ionosphere. This problem is best solved by using circular polarization, otherwise considerable care must be exercised in correctly accounting for the effect [Burns, 1970].

In summary, we found the moon to be a useful target for both power level verification and the absolute calibration of the Arecibo 430 MHz system. We suggest that if the moon is "visible" other radar systems such as the MST radar may be similarly calibrated. The level of error in comparing two different radars calibrated in this fashion would likely be ±2 dB. To do better than this would be difficult and probably expensive.

TABLE 1. VALUES OF C AND K USED IN EQUATION (4)

Wavelength	C	K	Reference
3.6 cm	21	3.573	Beckman [1965]
23 cm	62	1.9	*
68 cm	85	0.95	Beckman [1965]
6 m	165	0.03	Klemperer [1965]
10 m	190	0.0166	estimated

* Derived from 23 cm data given by Hagfors [1967, Table 1; 1970, Table 6].

TABLE 2. ARECIBO 430 MHz RADAR SYSTEM PARAMETERS FOR LUNAR CALIBRATION EXPERIMENT AND SIGNAL-TO-NOISE RATIO RESULTS

System	A	B
Antenna Gain	61.1 dBi	
Polarization	right circular – transmit	
	left circular – receive	
System Temperature [1]	339°K	
IF Filter Noise Bandwidth	9.78 kHz	
Pulse length	|← 2 msec	
Inter-Pulse Period	101.6 msec	
Pulse Shape	decaying exponential	
RC time constant	16 msec	30 msec
Pre-Receiver Attenuation	20.99 dB	71.59 dB
Nominal Transmitter Power	6 W	1.6 MW
Measured SNR[2]	5.5 ± .5	10.2 ± 1.0
Effective SNR[2] (No attenuation)	6.91(2) ± 9%	1.47(8) ± 9.8%
Absolute Received Power [2] (Watts)	3.16(-14) ± 9%	6.73(-9) ± 9.8%
Waveguide loss	0 dB	1.25 dB
Actual Transmitted Power (2% duty cycle)	5.9 W	1.26 MW(±19%)
Transmitter Power before losses	5.9 W	1.68 MW(±19%)

1 Attenuator (~290°K) plus front-end (~49°K) temperatures.

2 Based on an average of the pulse as described in the text.

TABLE 3. LUNAR SCATTERING CROSS-SECTION RESULTS FOUND USING EQUATION (A11) AND TABLE 2 PARAMETERS.

System	A	B
Nominal radar-subradar point distance R	3.674(5) km	
Lunar radius	1.7383(3) km	
Normalizing Integral Γ	1.430(-4)·πcr_ℓ	
Ratio $\overline{W}$ (square pulse)	0.516	
Ratio $\overline{W}$ (actual pulse)	0.479	0.496
Transmitted Power (Watts)	5.9	1.26(6)
Average Signal Power (Watts)	3.16(-14)±9%	6.73(-9)±9.8%
Inferred lunar cross-section (fraction of πr_ℓ^2)	0.054±9%	.051±9.8%

ACKNOWLEDGEMENTS

REFERENCES

Beckman, P. (196), Radar backscatter from the surface of the moon, *J. Geophys. Res.*, 70, 2345-2350.

Breakall, J. K. and J. D. Mathews (1982), A theoretical and experimental investigation of antenna near-field effects as applied to incoherent backscatter measurements at Arecibo, *J. Atmo. Terr. Phys.*, 44, 449-454.

Burns, A. A. (1970), On the wavelength dependence of radar echoes from the moon, *J. Geophys. Res.*, 75, 1467-1482.

Evans, J. V. and G. H. Pettengill (1963 a), The scattering behavior of the moon at wavelengths of 3.6, 68, and 784 centimeters, *J. Geophys. Res.*, 68, 423-447.

Evans, J. V. and G. H. Pettengill (1963 b), The radar cross-section of the moon, *J. Geophys. Res.*, 68, 5098-5099.

Evans, J. V. and T. Hagfors (1966), Study of radio echoes from the moon at 23 cm wavelength, *J. Geophys. Res.*, 71, 4871-4889.

Evans, J. V. (1969), Radar studies of planetary surfaces, *Ann. Rev. Astron. Astrophys.*, 7, 201-248.

Hagfors, T. (1967), A study of the depolarization of lunar radar echoes, *Radio Sci.*, 2, 445-465.

Hagfors, T. and J. V. Evans (1968), Radar studies of the moon, Chapter 5 in *Radar Astronomy*, McGraw-Hill, NY.

Hagfors, T. (1970), Remote probing of the moon by infrared and microwave emissions and by radar, *Radio Sci.*, 5, 189-227.

Harper, R. M. and W. E. Gordon (1980), A review of radar studies of the middle atmosphere, *Radio Science*, 15, 195-211.

Klemperer, W. K. (1965), Angular scattering law for the Moon at 6-meter wavelength, *J. Geophys. Res.*, 70, 3798-3800.

Kraus, J. D. (1950), *Antennas*, McGraw-Hill, NY.

Mathews, J. D. (1984), The incoherent scatter radar as a tool for studying the ionosphere D region, *J. Atmos. Terr. Phys.*, 46, 975-986.

Mathews, J. D. (1985), Incoherent scatter probing of the 60-100 km atmosphere and ionosphere, accepted IEEE Geosci. Remote Sensing.

Meyer, M. A. and H. G. Goldberg (1955), Applications of turnstile junction, *IRE Trans., Microwave Theory and Tech.*, 3, 40-45.

Prosser, R. T. (1965), The Lincoln calibration sphere, *Proc. IEEE*, 53, 1672.

Reisert, J. (1982), Requirements and recommendations for 70-cm Earth-Moon-Earth Communications, *Ham Radio Magazine*, 15, 12-19.

Rottger, J. (1980), Reflection and scattering of VHF radar signals from atmospheric refractivity structures, *Radio Sci.*, 15, 259-276.

Simpson, R. A. (1976), Surface roughness estimation at three points on the lunar surface using 23-cm monostatic radar, *J. Geophys. Res.*, 81, 4407-4416.

Simpson, R. A. and G. L. Tyler (1982), Radar scattering laws for the lunar surface, *IEEE Trans. Ant. Prop.*, AP-30, 438-449.

Stutzman, W. L. and G. A. Thiele (1981), *Antenna Theory and Design*, John Wiley & Sons, NY.

Thompson, T. W. (1979), A review of earth-based radar mapping of the moon, *The Moon and the Planets*, 20, 179-198.

Tyler, G. L. (1979), Comparison of quasi-specular radar scatter from the moon with surface parameters obtained from images, *Icorus*, 37, 29-45.

Reference is also made to the following unpublished material:

Breakall, J. K. (1983), On the absolute calibration and theoretical justification of high resolution ionosphere results obtained from Arecibo radar measurements, *Ph.D. Thesis*, Case Western Reserve University, Cleveland, OH.

APPENDIX A: ·

DERIVATION OF A LUNAR, TOTAL POWER, RADAR EQUATION

We require a form of the radar equation which relates on an absolute basis transmitted power to total (integrated over the relevant bandwidth) received power as a function of time as the radar pulse encounters and then traverses the moon. This radar equation will incorporate a general axially symmetric antenna pattern as well as a general radar pulse shape and duration. We assume in deriving this equation that the radar is "tracking" the lunar subradar point and that lunar scattering characteristics are axially symmetric about the line extending from the radar to the subradar point.

For the sake of simplicity in our final equation we take the origin of our time axis (t=0) to occur when the leading edge of the radar pulse arrives at the lunar subradar point. Thus, from Fig. A1 time t indicates the location of the radar pulse while time t' indicates "depth" into our location on the moon. Then a "square" radar pulse p(t',t) is given as:

$$p(t',t) = s(t' - t + \Delta) - s(t' - t) \qquad (A1)$$

where Δ is the pulse duration and s(t) is the unit step function (s(t≥0)=1; s(t<0)=0). A specific radar pulse shape is generated by multiplying the right hand side of (A1) by the appropriate normalized modulation term. As discussed in the main text we choose a decaying exponential with time constant τ_t (this does not restrict our final result). The net pulse $\gamma(t',t)$ is thus:

$$\gamma(t',t) = e^{-(t-t')/\tau_t} p(t',t) \qquad (A2)$$

where the leading edge of the pulse is located at $t' = t$ and the trailing edge at $t' = t-\Delta$.

The lunar radar "depth" τ_t corresponds to the time of propagation from the subradar point to the "center" of the moon and back again. The lunar radius is $r_\ell \equiv 1738.3$ km thus $\tau_t = 2r_\ell/c = 11.6$ msec where c is the speed of light. Thus a very short radar pulse would yield the "impulse response" of the moon and this response would fall to zero after 11.6 msec. The response from a pulse of duration Δ would fall to zero after 11.6 msec+Δ.

The radar energy flux (joules per square meter per second) at the moon is

$$\phi_\ell(t',t) = \frac{LP_o\gamma(t',t)G(\Theta(t'))}{4\pi R^2} \qquad (A3)$$

where L (≤1) is the transmitter/transmission line loss coefficient, P_o is peak transmitter power, R and Θ are defined in Fig. A1, and G is the antenna gain which we assume to be axially symmetric. In equation (A3) we assume the radar is tracking the lunar subradar point and that the range dependency of energy flux is negligible across the lunar radius. The energy flux given by (A3) illuminates the moon such that the high flux at the center of beam reflects from the region of the subradar point (i.e., $t'/\tau_\ell <<1$) while the smaller

fluxes away from the beam center illuminate annular regions at larger $t'/\tau_\ell, \alpha(t')$, or $\Theta(t')$. values as shown in Fig. A1. For a particular t' value it is readily shown that

$$\Theta(t') = \frac{\tau_\ell}{R} \sin \alpha(t') \qquad (A4)$$

$$\alpha(t') = \cos^{-1}(1 - t'/\tau_\ell)$$

We assume lunar surface radar scattering characteristics to be described in terms of $\sigma(\alpha(t))$ an isotropic scattering cross-section per unit surface area. From Fig. A1 the differential surface area of the annular ring at angle $\alpha(t')$ is $dS = 2\pi r_\ell^2 \sin\alpha d\alpha$ but from (A4) $d\alpha = dt'/\tau_\ell\sin\alpha$ thus

$$ds = \pi c r_\ell dt' \qquad (A5)$$

The projection of differential area dS onto the plane parallel to the illuminating wavefronts is $ds(\alpha)\cdot\cos\alpha$; thus the energy flux scattered back to the receiver is

$$d\phi_R(t', t) = \frac{\phi_\ell(t', t)\sigma(t')\pi c r_\ell dt'}{4\pi R^2} \qquad (A6)$$

The antenna effective area $A_e(= \lambda^2 G/4\pi)$, a measure of the antenna capability of converting an incident energy flux to available power at the receiver [Kraus, 1950; Stutzman and Thiele, 1981, section 1.10]) multiplied by (A6) yields the differential power received from the differential sized annular ring. Thus

$$dP_R(t', t) = \frac{\lambda^2 G(\Theta(t'))}{4\pi} d\phi_R(t', t) \qquad (A7)$$

and total received power is found by integrating over all t' from which different parts of the pulse contribute to the power received at time t. That is

$$P_R(t) = \frac{LP_o\lambda^2}{(4\pi)^3 R^4} \int_0^{\tau_\ell} e^{-(t-t')/\tau} [s(t' - t + \Delta) - s(t' - t)]G^2(\Theta(t'))\sigma(t')\cos\alpha(t')\pi c r_\ell dt' \qquad (A8)$$

where (A4) gives the relationship between t' and the angles $\Theta(t')$, $\alpha(t')$. Notice that having t' in (A8) in units of "roundtrip" travel time insures that the depth, $c\Delta/2$, from which energy in a pulse of duration Δ returns at any single instant is satisfied.

Equation (A8) may be put in more familiar terms by a renormalization procedure where

$$G(\Theta) = G_o P_n(\Theta) \qquad (A9)$$

$$\sigma(t')\cos\alpha(t') = \frac{\sigma_o \gamma_n(t')}{\Gamma}$$

and

$$\Gamma = \int_0^{\tau_\ell} \gamma_n(t')\pi c r_\ell dt' \qquad (A10)$$

16

In (A9) G_o is the maximum gain while $p_n(\Theta)$ is the normalized pattern. Also σ_o is the "widebeam–CW" lunar total scattering cross-section and γ_n is the normalized, short pulse total backscatter power (see eq. A14) or normalized scattering cross-section.

Application of eqs. (A9) and (A10) to (A8) yields

$$P_R(t) = \frac{\lambda^2 L P_o G_o^2 \sigma_o}{(4\pi)^3 R^4} \frac{1}{\Gamma} \int_0^{\tau_t} e^{-(t-t')/\tau_t} [s(t'-t+\triangle) - s(t'-t)] p_n^2(\Theta(t')) \gamma_n(t') \pi c r_\ell dt' \quad (A11)$$

The significant of σ_o becomes clear when we consider the CW (τ_t, $\triangle \rightarrow \infty$), wide beam ($p_n = 1$) form of (A11). In this limit (A11) becomes

$$P_R = \frac{\lambda^2 L P_o G_o^2}{(4\pi)^3 R^4} \sigma_o \quad (A12)$$

The significance of $\gamma_n(t')$ becomes apparent when we consider (A11) with $\tau_t \rightarrow \infty$, $p_n = 1$, and $\triangle \ll \tau_t$, then (A11) can be expressed as

$$P_R(t) = \frac{\lambda^2 L P_o G_o^2 \sigma_o}{(4\pi)^3 R^4} \cdot \frac{\gamma_n(t) \pi c r_\ell \triangle}{\Gamma} \quad (A13)$$

where we take γ_n to be constant across the "width" of the very short probing pulse. Thus $\gamma_n(t)$ can be measured using a short radar pulse combined with a wide beam antenna. That is dividing (A13) by $P_R(t=0+)$ (the leading edge peak power) gives

$$\gamma_n(t) = \frac{P_R(t)}{P_R(max)} \quad (A14)$$

which ultimately defined γ_n.

FIGURE CAPTIONS

Figure 1.   Received relative power is plotted versus time. Shown is a 51 second average (500 pulses) of the 2 msec long radar pulse scattered from the moon. This result was obtained using the 1.7 MWatt main 430 MHz transmitter. The baseline (lower solid line) corresponds to a 339°K system temperature and is found by averaging the noise in the entire 50 msec receiving "window" excluding the pulse region. The lower dashed line is the 5 standard deviation level of the baseline estimate. The average of the pulse peak region (upper solid line) is found using the 30 samples (50 μsec sampling interval) starting 0.5 msec into the pulse form the leading edge. The upper dashed lines are the 1 standard deviation level of the pulse peak estimate.

Figure 1A. Earth-radar/moon and radar pulse geometry.

Figure 2.   The normalized, short pulse, wide beam power (γ_n) and normalized antenna pattern squared (p_n^2) are plotted versus angle α expressed as lunar depth in time units (see (A4) and Fig. A1). The edge of the moon occurs at 11.8 msec. It is clear that γ_n initially decreases much more rapidly than p_n^2. Thus the subradar point appears as an angularly unresolved "bright spot" to the Arecibo 430 MHz system. The γ_n curve is the 68 cm result from Hagfors (1967,1970) while the antenna pattern is given by Mathews and Breakall (1982).

Figure 3.   The fully averaged and normalized received radar pulse with noise baseline removed is plotted versus time for the low power (a.) and high power (b.) transmitters. Also shown are the predicted pulse returns for the cases of an ideal (square) transmitter pulse and for decaying exponential pulses. The predicted returns are found using equations (A11) or (2) or (3) employing the data from Table 2 and Fig. 2 using transmitter time constants of infinity (ideal), 16 msec (a.), or 30 msec (b.). The quality of the predicted versus observed results indicates the basic correctness of the approach.
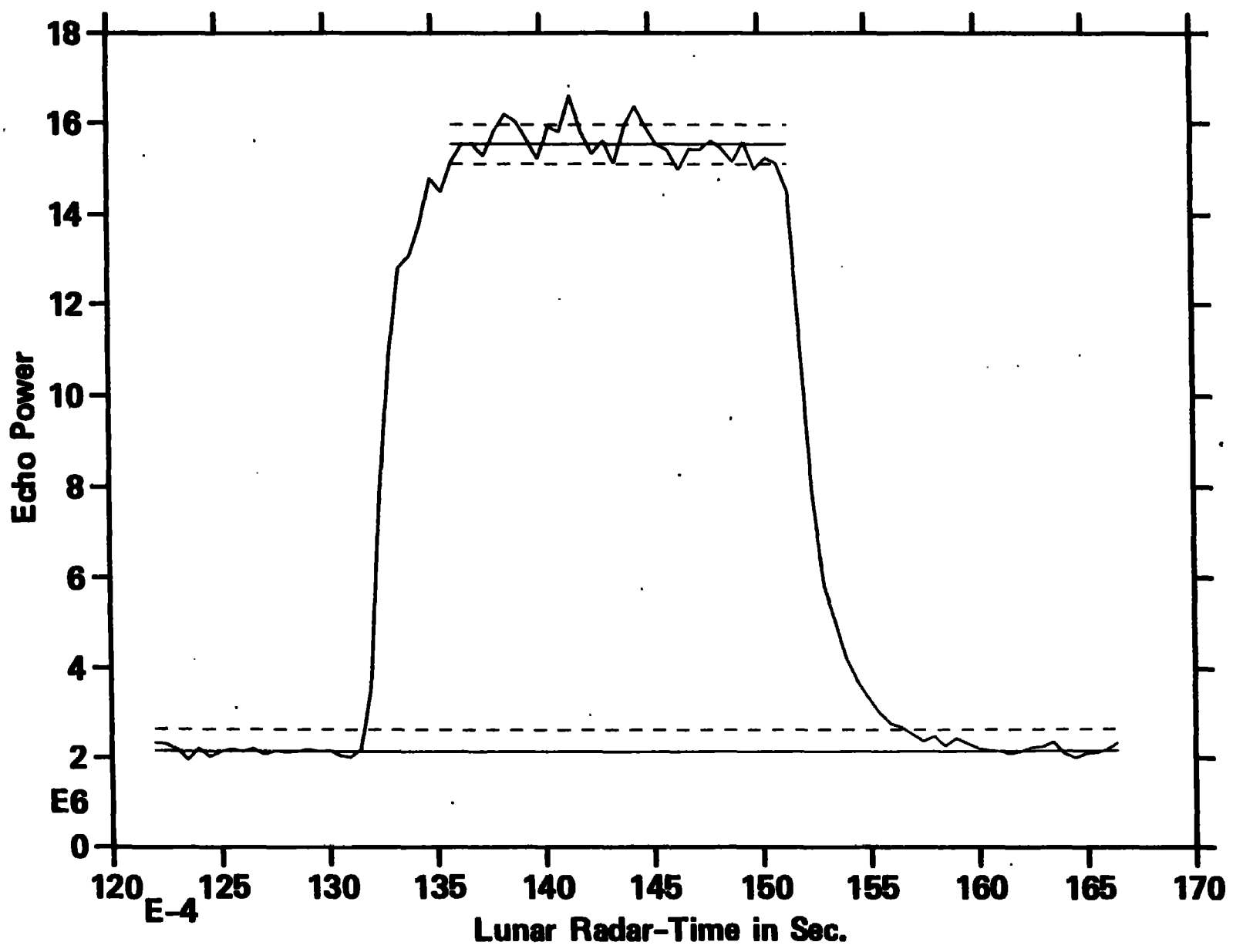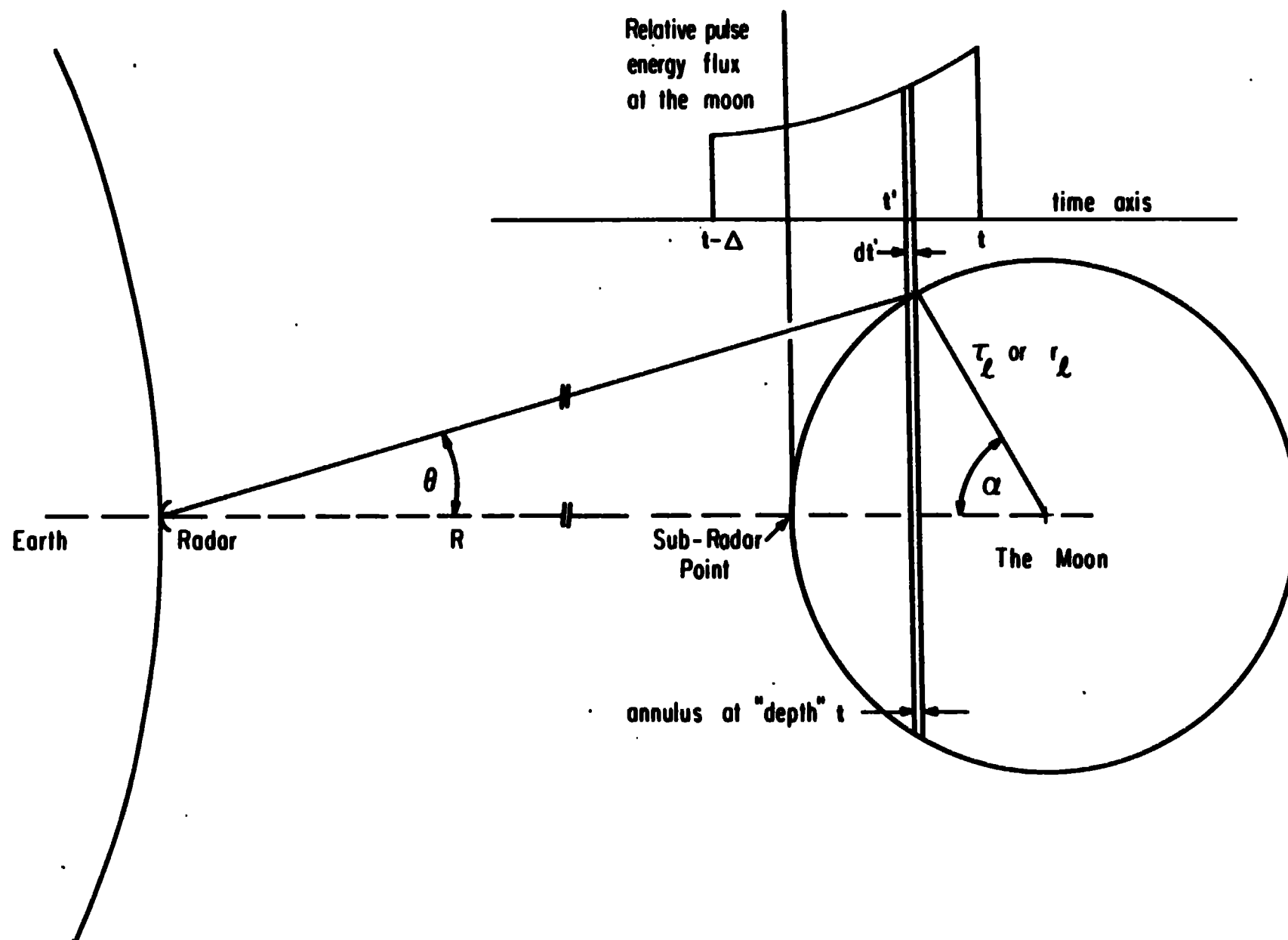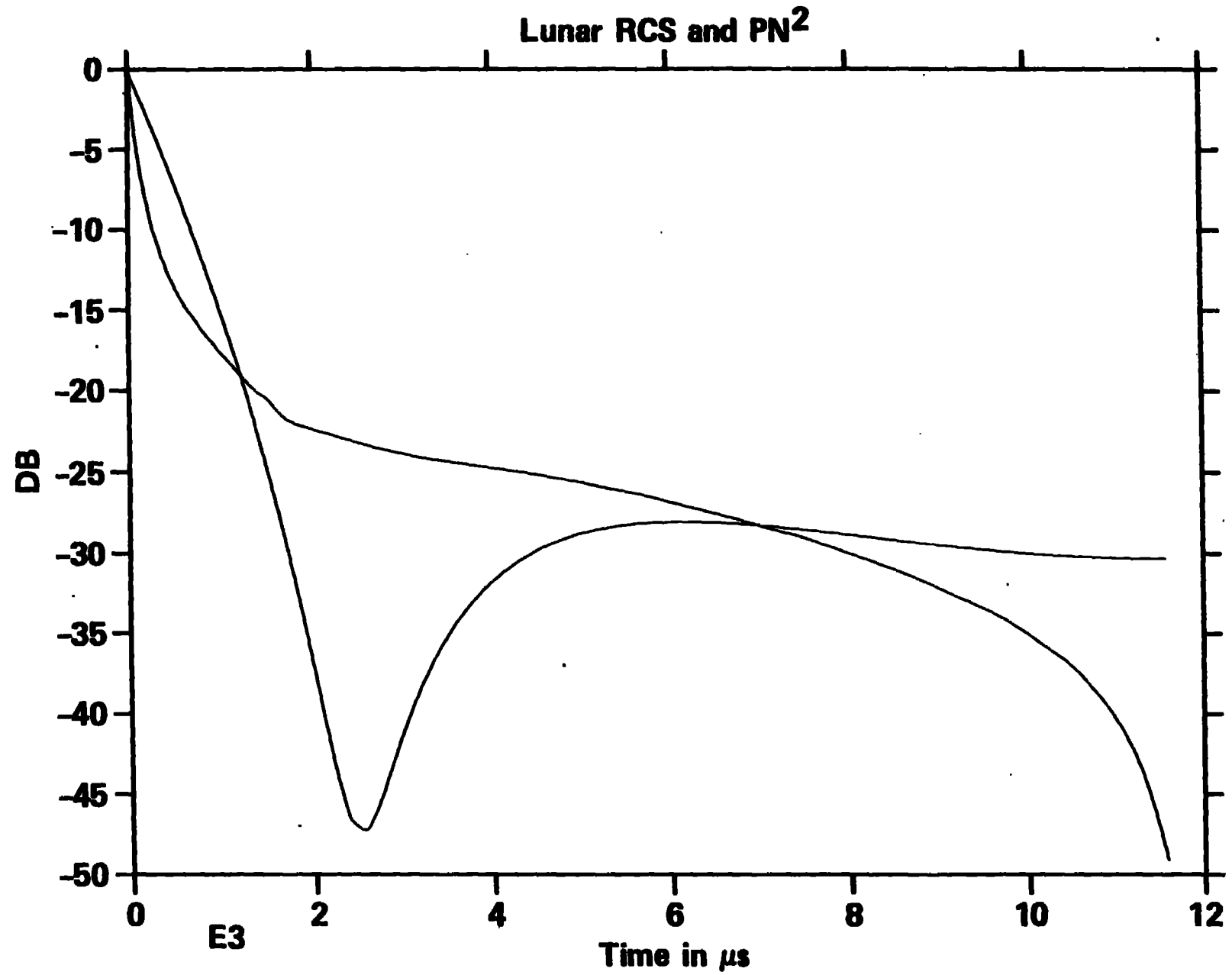
18

Fig. 1

fig. 1A

Relative pulse
energy flux
at the moon

time axis

$t-\Delta$ t' t

dt'

τ_ℓ or r_ℓ

θ

α

Earth   Radar   R   Sub-Radar   The Moon
                                Point

annulus at "depth" t

FIG2

Lunar RCS and PN^2

FIG3
B